Targeting the DNA damage response in cervical cancer

Wieringa, Hylke

ATR inhibition sensitizes cervical cancer cells for platinum-based chemoradiation

4

Hylke W. Wieringa[1], Marieke Everts[1], Malgosia Krajewska[1], Katarzyna K. Krzywicka[1], Mark A.J. Bastiaansen[1], Harry Hollema[2], G. Bea A. Wisman[4], Ate G.J. van der Zee[3], Elisabeth G.E. de Vries[1], Marcel A.T.M. van Vugt[1]

[1]Department of Medical Oncology, University Medical Center Groningen, University of Groningen, The Netherlands
[2]Department of Pathology, University Medical Center Groningen, University of Groningen, The Netherlands
[3]Department of Gynecological Oncology, University Medical Center Groningen, University of Groningen, The Netherlands

Manuscript in progress

Abstract

The cytotoxic effects of radiation and chemotherapy-induced DNA damage in cancer cells can be enhanced by inhibition of the 'DNA damage response' (DDR). Typically, DDR inhibitors are investigated either as monotherapy or in combination with a single DNA damaging agent. However, a number of solid tumors, including locally advanced cervical cancer (LACC), is treated with concomitant platin-based chemoradiation. How therapeutic targeting of the DDR can potentially be used in the context of chemoradiation is not clear.

In this study, we first explored the expression level and activation status of a panel of DDR kinases (ATR, Chk1, Chk2, DNA-PK and MK2) in a historical cohort of patients with stage IB-IVA disease treated either with primary radiotherapy (n=152) or chemoradiation (n=174). Immunohistochemical analysis of pre-therapy tumor samples demonstrated ubiquitous expression of ATR, Chk1, Chk2 and DNA-PKcs. High expression of activated DDR kinases was only observed for ATR and MK2. We also explored the relation between the expression and activation status of indicated DDR components and response to therapy and survival in the same tumor samples. Exploratory multivariate analyses showed that activated Chk1 was associated with a worse response-to-therapy (HR: 17.001; 95% CI: 2.258-128.030; *P*=0.006) and disease-specific survival (HR: 2.268; 95% CI: 1.058-4.860; *P*=0.035) in patients treated with chemoradiation.

We next investigated the chemoradiosensitizing potential of ATR/Chk1 inhibition. The aforementioned DDR kinases were chemically inactivated in a panel of cervical cancer cell lines (HeLa, SiHa, CSCC-7, CC-8, CC-11+ and CC-10B). Inhibition of DNA-PK, ATM or ATR sensitized cervical cancer cells for radiotherapy *in vitro*, whereas ATR and Chk1/2 inhibition sensitized cells for cisplatin treatment. ATR inhibition most effectively sensitized HeLa cervical cancer cells for platin-based chemoradiation.

Taken together, our exploratory analyses of cervical cancer tissues suggest that treatment of cervical cancer patients by chemoradiation may potentially be improved by additional inhibition of the ATR/Chk1 signaling axis. Our *in vitro* results confirm that inhibition of ATR indeed is a potentially effective way to sensitize cervical cancer cells for combined chemoradiotherapy.

Introduction

Radiotherapy combined with platinum-based chemotherapy is standard of care in locally-advanced cervical cancer (LACC) [1,2]. Nonetheless, this mode of treatment results in a 5-year overall survival rate of only 59.3% [3]. Development of novel agents to improve current standard of care is therefore needed. The cytotoxic effects of platinum-based chemotherapy and ionizing radiation are based on the induction of DNA damage. Ionizing radiation-induced cytotoxicity is mainly caused by creating of replication-independent DNA double strand breaks (DSBs) [4,5]. Cisplatin on the other hand, inflicts its cytotoxic effects in a replication-dependent manner via formation of inter- and intra-strand DNA crosslinks [6,7]. The beneficial effect of adding cisplatin to radiotherapy in cervical cancer treatment is generally thought to be caused by radiosensitization of tumor cells [6,10].

Modulation of the DNA damage response (DDR) machinery has been proposed to sensitize cervical cancer cells for cytotoxic agents [11,12]. The evolutionary conservated DDR signaling network detects and repairs (therapy-induced) DNA damage [13]. The DDR harbours a number of clinically actionable enzymes, including the kinases 'ataxia telangiectasia mutated' (ATM), 'ATM and Rad3-related' (ATR) and 'DNA-dependent protein kinase' (DNA-PK) [14-16]. Both ATM and DNA-PK are involved in processing DSBs, whereas ATR responds to single stranded (ss)DNA [14-17]. Activated ATM and ATR phosphorylate numerous substrates, including checkpoint kinase-2 (Chk2) and checkpoint kinase-1 (Chk1) [14,18]. In parallel, both ATM and ATR are involved in the activation of a more general stress-response pathway, consisting of p38 and mitogen-activated protein kinase-activated protein kinase-2 (MK2) [19]. Combined, activation of these DNA damage-induced pathways coordinates a cell cycle arrest with the initiation of DNA repair, and apoptosis in case of unrepairable damage [20].

Cervical cancer cells have a partially defective DDR pathway, due to human papilloma virus (HPV)-mediated inactivation of p53 and retinoblastoma 1 (RB1) [21,22]. As a result, these cells increasingly depend on residual cell cycle checkpoints, in particular the G_2/M checkpoint, for their survival in case of genotoxic stress [23,24].

Several DDR kinase inhibitors have been developed and have been tested for their ability to sensitize cancer cells either for ionizing radiation or for genotoxic chemotherapeutic agents [25]. However, DDR inhibitors are typically only tested in the context of single chemotherapeutic agents, or with ionizing radiation. Since chemoradiation is recommended for LACC patients, we here investigated how DDR inhibition can be optimally used to potentiate platinum-based chemoradiation in cervical cancer cells.

Results

Expression and activation status of DDR kinases in treatment-naïve cervical cancer tissue

To investigate the expression level and activation status of DDR kinases in LACC we immunohistochemically analyzed ATR, DNA-PKcs, Chk1, Chk2 and MK2 in pre-treatment tumor tissues. A historical cohort of patients with cervical cancer staged IB1 to IVA according to the Federation of Gynecologists and Obstetricians (FIGO) was analyzed, of which patient characteristics are described in Table 1. We analyzed nuclear expression of ATR, Chk1, Chk2, DNA-PKcs and MK2 in treatment-naïve tumor samples of 326 cervical cancer patients. Optimization of

immunohistochemical staining protocols is described in Supplemental Materials and Methods, Supplemental Table 1 and Supplemental Figure 2. Representative examples of immunostainings are shown in Figure 1B. Distributions of staining intensities are color-coded and show that all analyzed DDR kinases are abundantly expressed (Figure 1A and B). In 100% of the cases an IRS (immunoreactive score) of ≥ 5 was found for ATR and Chk1, while an IRS of ≥ 5 for DNA-PKcs and Chk2 was found in respectively 97.7% (n=251) and 99.6% (n=266) of the cases. Only MK2 was not abundantly expressed, with 24.1% of the tumors samples (n=60) showing low expression (IRS ≥ 5).

To determine the activation status of the indicated DDR kinases in tumors of treatment-naïve LACC patients, we analyzed phosphorylation status of kinases at residues that are known to reflect kinase activity (*i.e.* Ser-2056 on DNA-PKcs, Ser-345 on Chk1, Thr-68 on Chk2 and Thr-334 on MK2), or analyzed phosphorylation status of a substrate (*i.e.* Ser-33 on RPA32 as a read-out for ATR activity) [26-30]. Analysis of γ-H2AX was included to assess pretreatment levels of DNA damage. Representative immunohistochemical stainings of pRPA32, pDNA-PKcs, pChk2, pChk1 and pMK2 in 326 LACC patients are illustrated in Figure 1B. In treatment-naïve samples, only ATR and MK2 appeared to be active (IRS ≥5 in 76.1% and 92.2% of cases respectively). In contrast, DNA-PKcs, Chk1 and Chk2 were found to be infrequently activated, as more than 95% of cases showed IRS scores <5 (pDNA-PKcs: 95.2%, pChk1: 98.4% and pChk2: 96.9%) (Figure 1B). These findings likely represent few DNA breaks prior to treatment, as is underscored by low staining intensities for γ-H2AX, a marker of DNA DSBs (IRS <5 in 70.6% of cases, total n=175). As expected from kinase-substrate interactions, expression patterns of the individual kinases and their phosphorylated substrates were associated, as summarized, per treatment modality (Supplemental Table 4). Taken together, these results demonstrate that the indicated DDR kinases are abundantly expressed in LACC, which is a prerequisite for these kinases to serve as therapeutic targets.

Exploratory analysis of associations between DDR and disease-specific survival

We next performed an exploratory analysis to investigate the association between expression of DDR components in cervical cancer and disease-specific survival (DSS). Since distinct DDR kinases are involved in the cellular response to radiotherapy- and cisplatin-induced DNA damage, we performed subgroup analysis in patients who were primarily treated with radiotherapy (n=152) *versus* chemoradiation (n=174) (Table 2).

First, we assessed whether the abundance or phosphorylation status of indicated DDR components was associated with characteristics of cervical cancer patients, per treatment modality (for patient characteristics see Table 1). Baseline patient characteristics were similar for the two treatment regimens, except that patients treated with radiotherapy were older compared to the chemoradiation group (P<0.001). In the patient group primarily treated with radiotherapy (n=152), 92 patients died (60.5%), which was in 67 cases disease-specific. In the patients treated with chemoradiation (n=174), 76 (43.7%) patients died, of which 66 due to cervical cancer. Mann-Whitney U-test revealed less disease-specific deaths in the chemoradiation group compared to the radiotherapy group (P=0.002).

Second, multivariate analysis in the radiotherapy group showed that high pDNA-PKcs expression was independently associated with a worse disease-specific survival (DSS, HR

6.062; 95% CI 1.685-21.810; *P*=0.006). In contrast, high levels of Chk1 were related to a better DSS (HR 0.219; 95% CI 0.100-0.478; *P*<0.001) (Table 2). These results hypothesize for biological relevance of increased DNA-PKcs kinase activity in cervical cancer cells treated with radiotherapy. Multivariate analysis of the patient group treated with chemoradiation showed a different pattern of associations between DDR expression and DSS. In this group, pChk1 staining was related with a worse DSS (HR 2.268; 95% CI 1.058-4.860; *P*=0.035), whereas high MK2 expression (HR 0.439; 95% CI 0.249-0.772; *P*=0.004) was related with an improved DSS (Table 2). These results suggest that, if indeed Chk1 activity is causally related to these observations, that inhibition of Chk1 or its upstream activator ATR might be biologically relevant in cervical cancer cells treated with chemoradiation.

Table 1: Patient characteristics of 326 available tumor specimens of cervical cancer patients treated with combined radiotherapy and chemoradiation.

	Patients					
	All		Radiotherapy		Chemoradiation	
Variable	**N**	**%**	**N**	**%**	**N**	**%**
Patients	326		152		174	
Age at diagnosis (years)						
Median	54		65.6		47.4	
Range	21-92		27-92		21-82	
FIGO stage						
IB1	37	11.3	20	13.2	17	9.8
IB2	32	9.8	9	5.9	23	13.2
IIA	48	14.7	31	20.4	17	9.8
IIB	149	45.7	67	44.1	82	47.1
IIIA	7	2.1	3	2.0	4	2.3
IIIB	44	13.5	16	10.5	28	16.1
IVA	9	2.8	6	3.9	3	1.7
Histology						
Squamous	267	81.9	124	81.6	143	82.2
Adenocarcinoma	40	12.3	20	13.2	20	11.5
Other	19	5.8	8	5.3	163	6.3
Tumor grade						
Good/moderate	183	56.1	89	58.6	94	54.0
Poor	121	37.1	50	32.9	71	40.8
Missing	22	6.7	13	8.6	9	5.2
Lymphangio-invasion						
No	209	64.1	98	64.5	111	63.8
Yes	52	16.0	18	11.8	34	19.5
Missing	65	19.9	36	23.7	29	16.7
Tumor diameter						
0-4cm	87	26.7	46	30.3	41	23.6
≥4cm	216	66.3	91	59.9	125	71.8
Missing	23	7.1	15	9.9	8	4.6

n: number of patients; P: P-value; FIGO: International Federation of Gynecology and Obstetrics

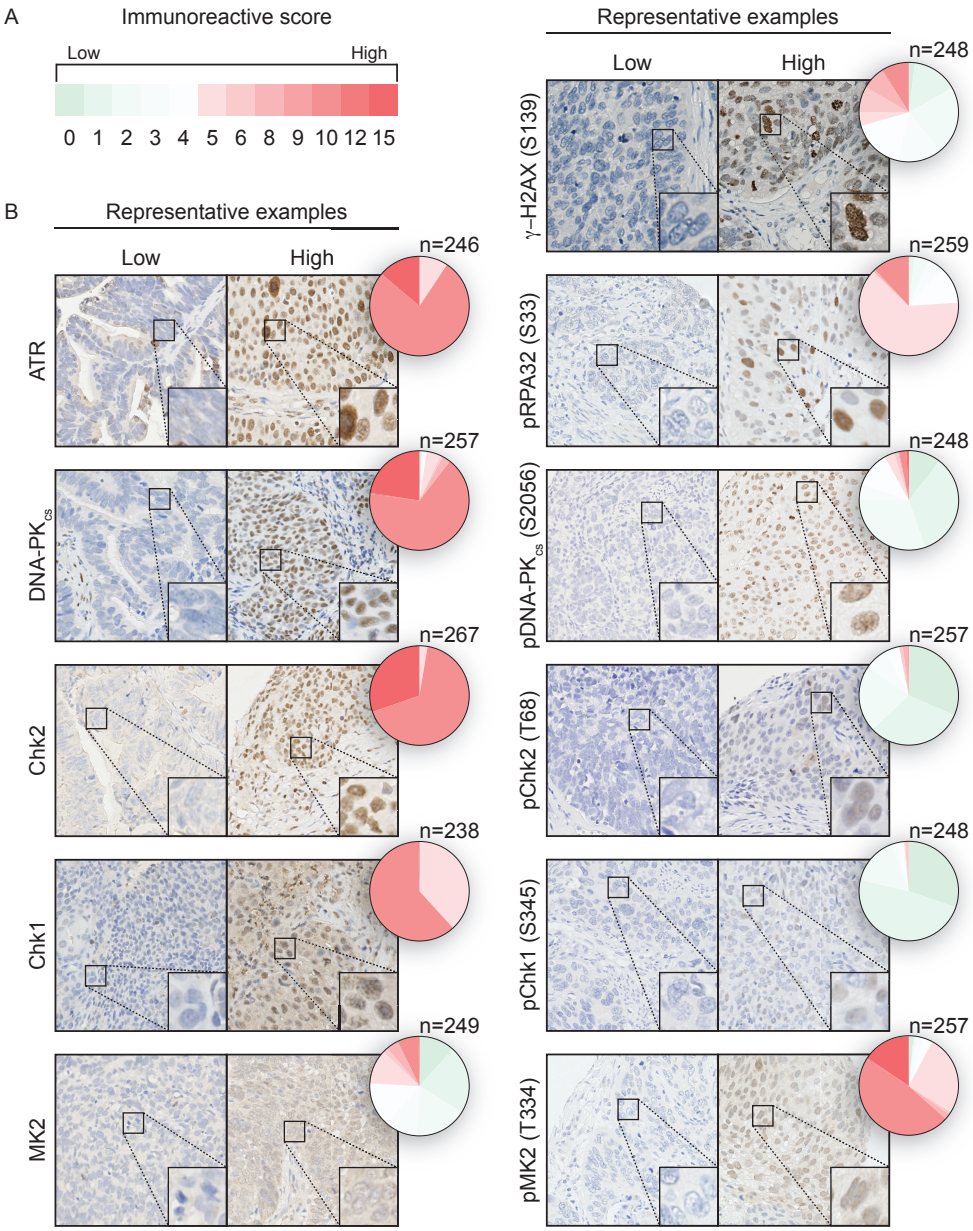

Figure 1: Representative stainings and distribution of IRS for DDR components in cervical cancer patients. ***(A)*** *Color-coding for the immunoreactive score (IRS) used for each staining. IRS consisted of percentage of positive stained tumor cells multiplied with the intensity of the staining.* ***(B)*** *Representative positive and negative/low staining for γ-H2AX, ATR, pRPA32, DNA-PKcs, pDNA-PK, Chk2, pChk2, Chk1, pChk1, MK2 and pMK2. Pie charts indicate IRS distribution for each staining. Numbers of patients included for statistical analysis are indicated above each pie chart. Magnifications used: 40x/80x.*

Table 2: Disease-specific survival analysis for γ-H2AX, ATR, pRPA32, DNA-PK$_{cs}$, pDNA-PK$_{cs}$, Chk1, pChk1, Chk2, pChk2, MK2, pMK2 expression levels in cervical cancer specimens of patients treated with either primary radiotherapy or primary chemoradiotherapy

	Radiotherapy						Chemoradiotherapy					
	Univariate			Multivariate			Univariate			Multivariate		
	HR	95% CI	*P*	HR	95% CI	*P*	HR	95% CI	*P*	HR	95% CI	*P*
Age (continuous)	0.994	0.980-1.009	0.415				0.997	0.979-1.016	0.748			
FIGO stage												
<IIB	*Ref.*						*Ref.*					
≥IIB	2.301	1.326-3.994	0.003	4.066	1.837-8.997	0.001	1.718	0.965-3.056	0.066	1.978	1.014-3.860	0.046
Histology			*0.250*						*0.035*			*0.016*
Squamous	*Ref.*						*Ref.*			*Ref.*		
Adenocarcinoma	1.457	0.776-2.736	0.242				2.001	1.067-3.751	0.031	2.976	1.403-6.311	0.004
Other	1.867	0.744-4.684	0.184				0.411	0.100-1.690	0.217	0.841	0.198-3.564	0.814
Tumor grade												
Good/moderate	*Ref.*						*Ref.*					
Poor	1.619	0.984-2.664	0.058	1.005	0.527-1.915	0.989	1.262	0.778-2.047	0.345			
Lymphangio-invasion												
No	*Ref.*						*Ref.*					
Yes	1.415	0.684-2.927	0.350				1.338	0.747-2.394	0.327			
Tumor diameter												
0-4 cm	*Ref.*						*Ref.*					
≥4 cm	2.359	1.280-4.347	0.006	2.425	1.142-5.151	0.021	1.583	0.860-2.914	0.140			
DDR components												
High γ-H2AX	0.937	0.480-1.828	0.849				1.639	0.700-3.839	0.255			
High ATR	0.591	0.278-1.257	0.172				1.306	0.519-3.286	0.571			
High pRPA32	1.310	0.617-2.779	0.482				1.206	0.436-3.336	0.718			
High DNA-PKcs	0.899	0.358-2.259	0.821				4.571	1.113-18.780	0.035	2.947	0.660-13.161	0.157
High pDNA-PKcs	3.008	0.935-9.674	0.065	6.062	1.685-21.810	0.006	1.062	0.423-2.670	0.898			
High Chk1	0.571	0.326-1.000	0.050	0.219	0.100-0.478	<0.001	1.198	0.671-2.139	0.541			
High pChk1	1.032	0.579-1.839	0.915				2.710	1.325-5.545	0.006	2.268	1.058-4.860	0.035
High Chk2	1.347	0.793-2.288	0.270				1.347	0.755-2.404	0.313			
High pChk2	1.110	0.629-1.962	0.718				0.898	0.520-1.550	0.698			
High MK2	0.767	0.437-1.348	0.357				0.480	0.279-0.824	0.008	0.439	0.249-0.772	0.004
High pMK2	1.218	0.686-2.160	0.501				1.418	0.791-2.540	0.241			

For multivariate analysis only variables were included with a P-value <0.010 in univariate analysis.
n: number; P: P-value; FIGO: International Federation of Gynecology and Obstetrics; HR: hazard ratio; 95% CI: 95% confidence interval.

Exploratory analysis of associations between DDR and response to therapy

To test whether inhibition of the ATR/Chk1-pathway could possibly be beneficial for the response to chemoradiation in LACC patients, we performed an exploratory analysis for associations between immunostainings and loco-regional disease-free survival, as a proxy for response-to-therapy, as previously described [31,32]. This retrospective analysis is based on the locoregional disease-free survival, which was defined as the time from diagnosis of disease until clinical locoregional disease progression during therapy or locoregional recurrence after completion of therapy [31,32]. Patients with an unknown location of recurrence were excluded for analysis (n=10; 3.1%).

In the multivariate analysis for LACC patients who were primarily treated with radiotherapy (Table 3), high expression levels of Chk2 were associated with an increased HR of 2.748 (95% CI 1.077-7.016; *P*=0.035) for locoregional progression or recurrence of LACC (Table 3). In the multivariate analysis for LACC patients treated with chemoradiation (Table 3), high expression levels of pChk1 were related with a worse locoregional disease free survival (HR 17.001; 95% CI 2.258-128.030; *P*=0.006). In addition, high expression levels of pChk2 (HR 0.375; 95% CI 0.168-0.839; *P*=0.017) or MK2 (HR 0.352; 95% CI 0.156-0.791; *P*=0.011) were related to an improved locoregional disease free survival.

These data may imply that different signaling axes within the DDR control the response to radiotherapy *versus* chemoradiation, and that differential DDR targeting strategies may be required to potentiate these different treatment modalities.

Table 3: Exploratory response to therapy analysis for γ-H2AX, ATR, pRPA32, DNA-PK$_{cs}$, pDNA-PK$_{cs}$, Chk1, pChk1, Chk2, pChk2, MK2, pMK2 expression levels in cervical cancer specimens of patients treated with either primary radiotherapy or primary chemoradiotherapy

	Radiotherapy						Chemoradiotherapy					
	Univariate			Multivariate			Univariate			Multivariate		
	HR	95%CI	P	HR	95%CI	P	HR	95%CI	P	HR	95%CI	P
Age (continuous)	1.011	0.988-1.035	0.351				1.002	0.977-1.028	0.863			
FIGO stage												
<IIB	*Ref.*						*Ref.*					
≥IIB	2.170	0.959-4.909	0.063	1.464	0.563-3.806	0.434	1.343	0.621-2.904	0.454			
Histology			*0.136*			*0.010*						
Squamous	*Ref.*			*Ref.*			*Ref.*					
Adenocarcinoma	1.538	0.580-4.080	0.387	1.340	0.455-3.949	0.596	1.782	0.681-4.665	0.239			
Other	3.265	0.972-10.969	0.056	8.486	2.120-33.971	0.003	0.874	0.206-3.704	0.855			
Tumor grade												
Good/moderate	*Ref.*						*Ref.*					
Poor	1.503	0.710-3.180	0.287				1.706	0.847-3.435	0.135			
Lymphangio-invasion												
No	*Ref.*						*Ref.*					
Yes	1.016	0.299-3.452	0.979				0.903	0.364-2.237	0.825			
Tumor diameter												
0-4 cm	*Ref.*			*Ref.*			*Ref.*					
≥4 cm	2.074	0.884-4.865	0.093	1.415	0.497-4.028	0.516	1.739	0.713-4.239	0.224			
DDR components												
High γ-H2AX	0.935	0.344-2.539	0.895				2.368	0.559-10.037	0.242			
High ATR	0.163	0.022-1.215	0.077	0.146	0.019-1.127	0.065	0.435	0.059-3.205	0.414			
High pRPA32	0.840	0.311-2.270	0.730				1.088	0.257-4.600	0.908			
High DNA-PKcs	2.352	0.317-17.483	0.403				4.099	0.555-30.263	0.167			
High pDNA-PKcs	2.014	0.469-8.645	0.346				2.483	0.336-18.359	0.373			
High Chk1	0.516	0.223-1.197	0.124				0.887	0.398-1.981	0.771			
High pChk1	1.303	0.509-3.337	0.581				5.698	1.345-24.140	0.018	17.001	2.258-128.030	0.006
High Chk2	2.113	0.949-4.706	0.067	2.748	1.077-7.016	0.035	0.544	0.188-1.570	0.260			
High pChk2	1.275	0.520-3.128	0.596				0.487	0.225-1.052	0.067	0.375	0.168-0.839	0.017
High MK2	0.716	0.300-1.712	0.453				0.492	0.227-1.064	0.072	0.352	0.156-0.791	0.011
High pMK2	0.728	0.319-1.664	0.452				1.391	0.609-3.180	0.434			

For multivariate analysis only variables were included with a P-value <0.010 in univariate analysis.
n: number; P: P-value; FIGO: International Federation of Gynecology and Obstetrics; HR: hazard ratio; 95% CI: 95% confidence interval.

Cell cycle abrogation upon DDR inhibition

To test whether inhibition of various DDR kinases has differential effects on DNA damage responses in cervical cancer cells, we assessed cell cycle progression in response to irradiation. Asynchronous HeLa cells were analyzed at several time points after 5 Gy irradiation, and if indicated, DDR kinase inhibitors were added 1 hour prior to irradiation (Figure 2A, B). Irradiation of control-treated cells resulted in a clear G_1/S and G_2/M checkpoint arrest, as based on DNA content analysis and phospho-Histone-H3 (p-HH3) staining to quantify mitotic cells (Figure 2A). Inhibition of ATM or DNA-PK resulted in an override of the irradiation-induced G_1/S checkpoint override and lead to an accumulation of cells in the G_2-phase (Figure 2A, B). In contrast, inhibition of ATR or combined Chk1/2 inhibition resulted in a clear override of the G_2/M checkpoint arrest, whereas inhibition of MK2 did not result in obvious checkpoint malfunction after irradiation (Figure 2A, B). So, the G_1/S and G_2/M checkpoints show differential requirements concerning DDR kinases after ionizing radiation.

To test whether loss of DDR function due to checkpoint kinase inhibition was accompanied with elevated levels of apoptosis, we analyzed sub-G_1 DNA content [33]. Interestingly, Chk1/2 inhibition, but not ATR inhibition, resulted in an increased sub-G_1 fraction in irradiated cells (Figure 2C and Supplemental Figure 2B). So, in contrast to our observation that both Chk1/2 and ATR inhibition result in a dysfunctional G_2/M cell cycle checkpoint, only Chk1/2 inhibition resulted in elevated levels of apoptosis.

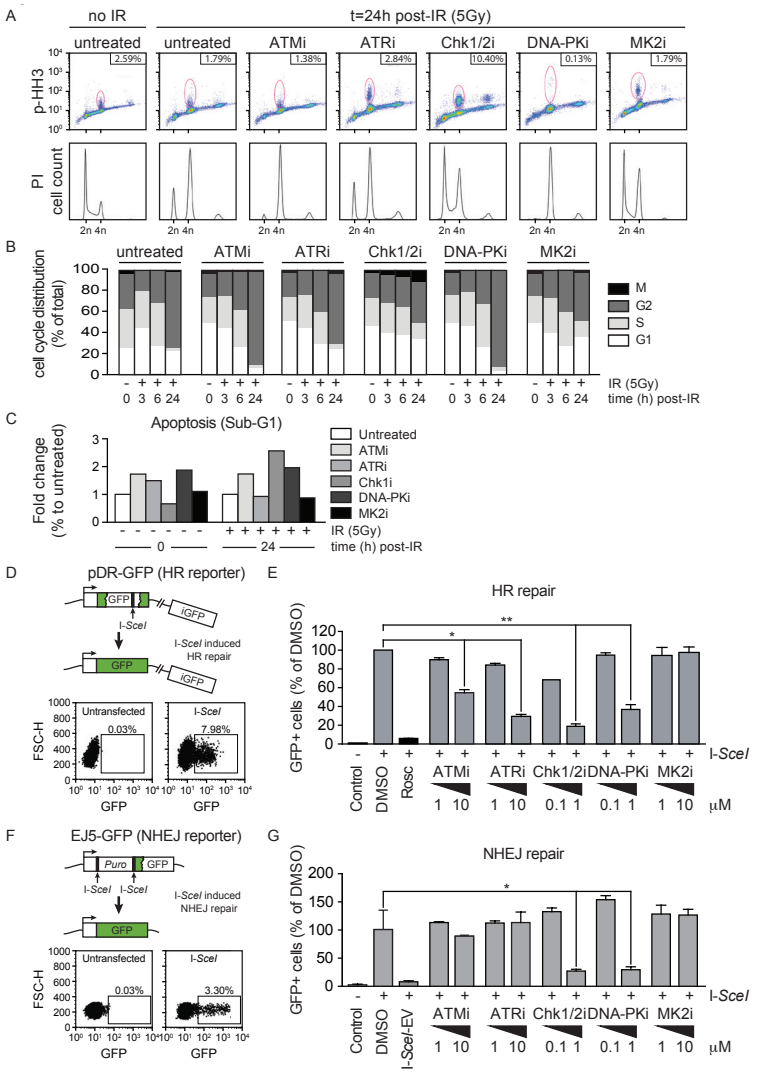

Figure 2: Effects of specific DDR-inhibition on cell cycle checkpoints capacity and HR and NHEJ repair. (A-C) *HeLa cells were 1 hour prior to irradiation (5 Gy) treated with 10 μM KU55933 (ATMi), 10 μM NU6027 (ATRi), 0.1 μM AZD7762 (Chk1/2i), 1 μM KU0060648 (DNA-PKi), 10 μM MK2 inhibitor III (MK2i). At indicated time points (0, 3, 6, 24 hours) cells were harvest, fixated and stained for PI/RNAse and p-HH3. At least 10,000 events were analyzed per sample. Representative DNA plots 24 hours after irradiation (5 Gy) are shown in* ***(A)****. In* ***(B)*** *cell cycle distribution*

of HeLa cells 0, 3, 6, and 24 hours after ionizing irradiation (IR). In ***(C)*** *the fold change compared to the untreated condition of HeLa cells in sub-G_1 are shown for HeLa cells before treatment (t = 0h) and 24 hours after IR (5Gy). Results are from one independent experiment.* ***(D)*** *Schematic representation of the homologous recombination (HR) repair assay. The pDR-GFP reporter (top) was previously stably transfected into HeLa cells {36:2015ii}. In case of HR repair, the GFP gene is repaired after the I-Sce1-induced DNA double-strand break in the GFP gene, resulting in GFP+ cells. Subsequently, this was quantified by flow cytometry (bottom).* ***(E)*** *Monoclonal HeLa-pDR-GFP cells were 1 hour after transfection with I-Sce1 endonuclease treated with control treatments (DMSO = positive control; Roscovitine = negative control) or two different concentrations of the indicated DDR inhibitors (ATMi, ATRi, Chk1/2i, DNA-PKi, MK2i). After 48 hours, cells were analyzed for their GFP+ with flow cytometry. At least 10,000 cells per condition were counted. GFP+ was related to the DMSO control. Averages and standard deviation (SD) are the result from three independent experiments.* ***(F)*** *Schematic representation of the non-homologues end-joining (NHEJ) repair assay. The EJ5-GFP reporter (top) was kindly provided by Dr. Jeremy Stark. We stably transfected the EJ5-GFP reporter into HeLa cells, selected cells in puromycin (1 µg/mL). The EJ5-GFP reporter consists of a GFP gene in which the promotor and the GFP coding region are separated by a I-Sce1- flanked puromycin cassette. A DNA DSB is introduced by I-Sce1 and, in case of NHEJ repair, will lead to restoration of functional GFP gene (top). Subsequently, this was quantified by flow cytometry (bottom).* ***(G)*** *DMSO treatment 1 hour after transfection with I-Sce1 endonuclease was used as positive control, whereas transfection with an I-Sce1-EV (empty vector) served as negative control for the NHEJ repair assay. Monoclonal HeLa-EJ5-GFP cells were 1 hour after transfection with I-Sce1 endonuclease treated with two different concentrations of DDR inhibitors (ATMi, ATRi, Chk1/2i, DNA-PKi, MK2i). After 48 hours, cells were analyzed for their GFP+ with flow cytometry. At least 10,000 cells per condition were counted. GFP+ was related to the DMSO control. Averages and standard deviation (SD) are the result from three independent experiments.*
*p-HH3 = phospho-Histone-H3, PI = propidium iodide, Rosc = roscovitine, *P <0.05, **P <0.01,*

Effects of DDR kinase inhibition on DNA repair

To study the effects of DDR kinase inhibition on the capacity to repair DNA double strand (DSB) breaks, we utilized two fluorescence-based reported systems. The pDR-GFP reporter was used to assess homologous recombination repair (HRR), whereas the EJ5-GFP reporter was used to assess non-homologous end-joining (NHEJ) repair [34,35]. Upon induction of an I-Sce1-induced DSB break in the pDR-GFP reporter, GFP expression is only induced after restoration of the GFP reading frame by HRR (Figure 2D). As expected, treatment with the CDK inhibitor roscovitine precluded GFP expression, as CDK activity is required for HRR (Figure 2E) [36]. Notably, a reduction in HRR was observed upon inhibition of ATM, ATR, Chk1/2 or DNA-PK inhibition, when compared to DMSO-treated cells (Figure 2E).

To assess NHEJ efficiency, HeLa cells harboring the EJ5-GFP NHEJ reporter were treated with indicated DDR inhibitors (Figure 2G). As expected, inhibition of DNA-PK reduced the percentage of GFP-positive cells after I-Sce1 transfection. Whereas ATR and ATM inhibition did not notably alter NHEJ, treatment with the Chk1/2 inhibitor surprisingly resulted in a significant ($P<0.05$) reduction in NHEJ efficiency (Figure 2G).

ATR/Chk1/2 inhibition sensitizes cervical cancer cells to cisplatin

To determine which of the selected DDR kinase inhibitors most efficiently potentiated the cytotoxic effects of cisplatin, we performed short-term survival assays in a panel of cervical cancer

cell lines. HeLa and SiHa cells as well as early-passage cervical cancer cell lines CSCC-7, CC-8, CC-11+ and CC-10B were treated with increasing concentrations of cisplatin, in combination with indicated DDR-inhibitors. Treatment with the Chk1/2 inhibitor AZD7762 sensitized all tested cervical cancer cell lines to cisplatin (Figure 3A, B, Supplemental Table 5). These effects could be attributed to Chk1 inhibition, as a dedicated Chk2 inhibitor did not notably increase cisplatin-induced cytotoxicity (data not shown). Inhibition of ATR with the compound NU6027 also sensitized the majority of the cell lines, except for the CC-11+ cell line (Figure 3A). In contrast, increased cytotoxicity was not invariably observed when cisplatin was combined with inhibitors of ATM, DNA-PK or MK2 (Figure 3A, B, Supplemental Table 5).

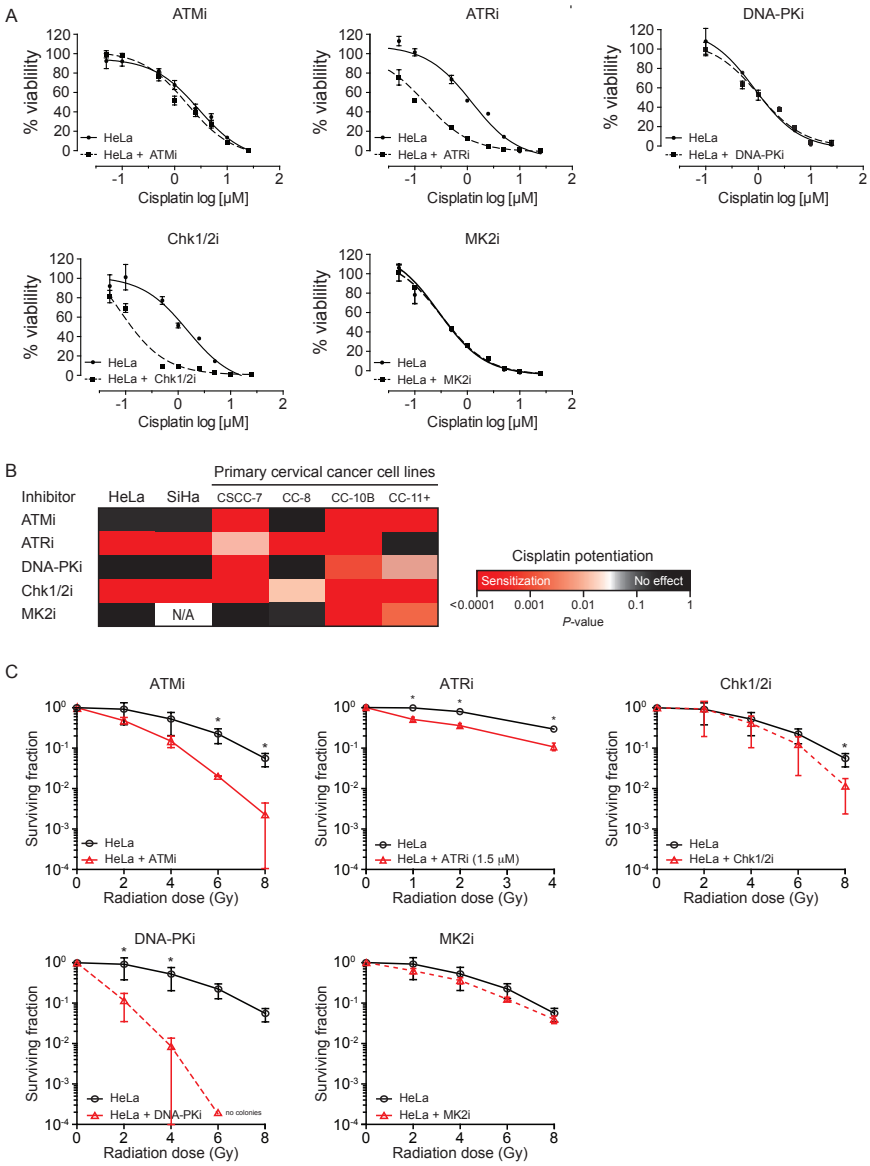

Figure 3: Potentiation for cisplatin or ionizing radiation by DDR inhibitors in cervical cancer cells.*To study sensitization to cisplatin by DDR inhibitors we performed a short-term survival assay. For potentiation of ionizing radiation a clonogenic survival assay was performed.* ***(A)*** *HeLa cells were treated with indicated concentrations of cisplatin in combination with control (DMSO or H2O) or indicated DDR inhibitor treatment. After 4 days of treatment, cells were incubated with MTT and cell viability was performed by colorimetric measurement. DDR inhibitors included: 10 μM KU55933 (ATMi), 10 μM NU6027 (ATRi), 0.1 μM AZD7762 (Chk1/2i), 1 μM KU0060648 (DNA-PKi), 10 μM MK2 inhibitor III (MK2i).* ***(B)*** *Heat map illustrating P-values from the extra sum-of-square F-test to test the difference in the MTT-curves between control and DDR inhibitor. Red indicates a significant sensitization (survival curve) to cisplatin by the specific DDR inhibitor compared to its control treatment. VE821 was used as a second specific ATR inhibitor to confirm the effects seen by NU6027 (ATRi) treatment.* ***(C)*** *HeLa cells were plated in 6-wells plates, pretreated with control (DMSO or H2O) or indicated DDR inhibitor treatment for 1 hour and irradiated with indicated doses (0-8 Gy). DDR inhibitors included: 10 μM KU55933 (ATMi), 10 μM NU6027 (ATRi), 0.1 μM AZD7762 (Chk1/2i), 1 μM KU0060648 (DNA-PKi), 10 μM MK2 inhibitor III (MK2i). After 10-12 days colonies were fixed in methanol and subsequently stained using Coomassie Brilliant Blue. Numbers of colonies (>50 cells per colony) were related to number of plated cells to calculate survival fractions. The surviving fractions of non-irradiated cells were used as a reference. Student's T-test was used to test significant differences. In case of ATRi, use of 10 μM NU6027 in combination with high doses of ionizing radiation resulted in no colony formation. To demonstrate a gradual radiopotentiation of ATR inhibition, we evaluated three different concentrations of ATRi (0.5, 1.0, 1.5 μM) in combination with lower doses of ionizing radiation (0-4Gy).*
*P-values <0.05 were considered as significant. *P <0.05, § P <0.05.*

Radiosensitization through inhibition of ATM, ATR or DNA-PK

We subsequently analyzed whether the indicated DDR inhibitors induced radiosensitizing effects in long-term clonogenic survival assays. In HeLa cells, inhibition of ATM, ATR or DNA-PK resulted in a reduction in clonogenic survival at all tested doses of ionizing radiation (Figure 3C). Treatment with the Chk1/2 inhibitor only decreased cell survival at a high dose ionizing radiation (8 Gy), whereas inhibition of MK2 did not alter clonogenic survival (Figure 3C). Combined, our results demonstrate a differential required for DDR kinases in the context of cellular survival after cisplatin treatment *versus* radiation.

Sensitization to combined radiochemosensitivity

As potentiation of cisplatin versus radiotherapy required inactivation of different DDR kinases, this poses a challenge when DDR kinase inactivation is considered as a strategy for improving combined radio-chemotherapy. To assess which DDR kinase should be inactivated to most potently increase the cytotoxic effects of combined treatment of cisplatin with radiotherapy, we assessed clonogenic survival after combined treatment with cisplatin and irradiation. Twenty-four hours after plating, cells were treated with the indicated DDR-inhibitors, after which cisplatin was added for 8 consecutive hours. After careful wash out of the cisplatin-containing medium, cells were irradiated with indicated doses in the presence of DDR inhibitors. As the cytotoxicity of combined treatment with cisplatin and irradiation was higher when compared to single treatments, we used a lower radiation doses and lower concentrations of cisplatin (1 μM) in these assays.

In line with our earlier results, we did not observe potentiating effects towards combined treatment with irradiation and cisplatin upon MK2 inhibition in HeLa cells (Figures 4A, 3A, C). As observed earlier, inhibition of ATM or DNA-PK effectively sensitized to irradiation, but did not cause additional sensitization in the presence of cisplatin (Figure 4A). Also Chk1/2 inhibition did not significantly demonstrate additive chemo-radiosensitizing effects, whereas it did potentiate cells to single cisplatin treatment (Figure 4A). In contrast, inhibition of ATR strongly potentiated the combined cisplatin-based chemoradiation and completely prevented clonogenic survival (Figure 4A). These data indicate that ATR inhibition may constitute a powerful therapeutic approach to potentiate cisplatin-based chemoradiotherapy.

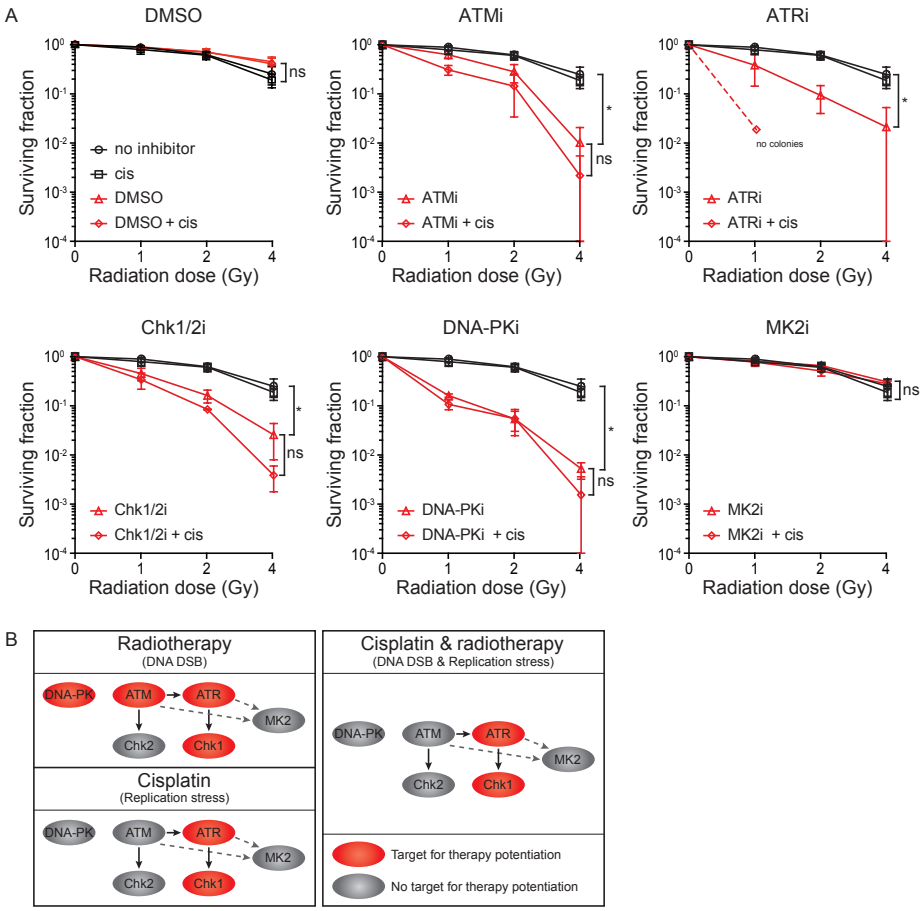

Figure 4: Inhibition of ATR chemoradiosensitizes HeLa and CC-10B cervical cancer cells. (A) *HeLa cells were plated in 6-wells plates, pretreated with control (DMSO) or indicated DDR inhibitor treatment for 30 minutes, incubated with cisplatin for 8 hours, and irradiated with indicated doses (0-8 Gy). DDR inhibitors included: 10 μM KU55933 (ATMi), 10 μM NU6027 (ATRi), 0.1 μM AZD7762 (Chk1/2i), 1 μM KU0060648 (DNA-PKi), 10 μM MK2 inhibitor III (MK2i). After 10-12 days colonies were fixed in methanol and subsequently stained using Coomassie*

*Brilliant Blue. Numbers of colonies (>50 cells per colony) were related to number of plated cells to calculate survival fractions. The surviving fractions of non-irradiated cells were used as a reference. One-way ANOVA test was used to test significant differences. P-values <0.05 were considered as significant. *P <0.05.* ***(B)*** *Graphical illustration of the importance to distinguish between targets that can be used to potentiate cervical cancer cells for radiotherapy (left panel), cisplatin (left panel) or combined cisplatin and radiotherapy (right panel). Kinases in red are suitable to cause potentiation in HeLa cells for the corresponding type of DNA damage. Grey indicates kinases that are not demonstrated to result in potentiation upon inhibition in HeLa cells.*

Discussion

In this report we have investigated the expression and activation status of key DDR components in pre-treatment tumor tissue of stage IB to IVA cervical cancer patients. We showed that the DDR components ATR, DNA-PKcs, Chk2 and Chk1 are abundantly expressed in the vast majority of tumor tissues, whereas only MK2 demonstrated more variation in expression and was lowly expressed in a subset of tumors. Concerning the activation status of indicated DDR components, only ATR showed high levels of activity in pre-treatment tissues, judged by the phosphorylation status of its substrate RPA32. Importantly, we found that *in vitro* only pharmacological inhibition of ATR could sensitize cervical cancer to cisplatin-based chemoradiation.

Concerning the expression of DDR components in cervical cancer, the amount of data is very limited. DNA-PKcs has shown to be up-regulated in early-stage cervical cancer patients, while no associations between DNA-Pkcs expression levels and patient survival were found [37]. This is in line with our observation of DNA-PKcs expression levels, in which high DNA-PKcs expression was more frequently observed in an advanced stage (>IIB) cervical cancer (P=0.044) and did not relate with DSS (Table 2). Analysis of the abundance of Chk1 and expression of pChk1 was immunohistochemicaly analyzed in stage IB-IIA cervical cancer tissues (n=147) and normal epithelial tissues (n=74) showed that both Chk1 and pChk1 were elevated in cervical cancer, although predictive or prognostic impact of these findings were not reported [38]. Our data showed abundant Chk1 expression, while ~30% of tumor tissues were negative for pChk1. The only DDR components that showed activity in pre-treatment tissue were ATR and MK2. Phosphorylation of the RPA complex, primarily results from phosphorylation on residue S33 of subunit RPA32 by ATR, and likely reflects elevated levels of replication stress [39]. Concerning MK2, this kinase functions in parallel to Chk1 and DNA damage, and was shown to function in p53-deficient cancer cells as a checkpoint kinase for G_1, S and G_2/M cell cycle checkpoints [40]. Immunostaining of pMK2 was previously only reported for normal tissues and thyroid carcinomas [41]. In these reports, pMK2 (and MK3) expression was mostly cytoplasmic and was elevated in cancerous tissue compared to normal tissue [41]. In a previous study, we showed that high levels of phosphorylated ATM on residue Ser-1981 were related with a worse DSS [31]. We realize that the patient material that we analyzed in this study is from a historical cohort, rather than a preferred prospective study [42]. However, despite the use of a single TMA of a retrospective cohort analysis, this study adds to our knowledge of the abundance and activation status of DDR components in pre-treatment cervical cancer tissue.

In literature, the DDR has been proposed to act as a barrier to prevent carcinogenesis in

various cell types [43,44]. Key DDR pathways, including p53, ATM and Chk2 become activated in pre-cancerous tissues to prevent progression to more malignant stages [43,44]. Partial (epi) genetic inactivating of the DDR machinery is therefore thought to be essential for transformation of human dysplastic cells to cancerous cells [43-45]. Mostly, mutational loss of TP53 facilitates this step [43,44]. In cervical cancer p53 is already compromised by persistent HPV infection, which could explain why key DDR components, including ATM, 53BP1 and Chk2, remain unaltered in cervical cancer tissues. The observation that the indicated DDR components are almost invariably expressed in cervical cancer is relevant in the context of therapeutic inactivation of the DDR, for which target expression is required.

Based on our data, we propose inhibition of ATR as an interesting DDR target to potentiate the current treatment modality of cisplatin treatment with radiation in locally advanced cervical cancer. So far, most studies in which DDR-targeting compounds are studied assess their effects only in combination with a single therapeutic agent, typically only cisplatin or ionizing radiation. To mimic the clinical situation, we therefore tested DDR inhibitors in the context of combined chemo-radiotherapy. The recent development of more selective and potent ATR inhibitors has enabled the further exploration of the therapeutic potential of ATR inhibition. Notably, the reversible ATR inhibitor ETP-46464 demonstrated a prominent radiosensitizing effect in breast cancer cells [46], and the NU6027 ATR inhibitor showed potentiation of the cytotoxic effects of ionizing radiation and cisplatin in breast and ovarian cancer cell lines [47]. Despite these studies, *in vivo* results with ATR-targeting therapeutics are currently limited. This may be due to unfavorable pharmacokinetics of the available compounds. Although results in cervical cancer models have not been reported, the recent ATR inhibitors AZ20, VX-790 and AZD6738 are compatible with *in vivo* use, and are currently tested in clinical trials (NCT02264678, NCT02223923, NCT01955668) [48,49].

Interestingly, sensitizing effects of ATR inhibition towards chemoradiotherapy *in vivo* were observed preferentially in p53-deficient tumors [49], underscoring the potential impact for cervical cancer. Studies combining these novel compounds with cisplatin-based chemoradiotherapy in cervical cancer using *in vivo* models and clinical studies are therefore warranted to explore ATR inhibitors for improving cervical cancer treatment.

Materials and Methods

Patient group and immunohistochemistry

Treatment-naïve tumor tissue of cervical cancer patients (n=326), diagnosed between January 1980 and December 2006 in the University Medical Center Groningen (UMCG) and affiliated hospitals, were processed for tissue microarray (TMA) assembly as decribed previously [31,32]. For patient flow chart and detailed information see Supplemental Figure 1 and Supplemental Materials and Methods. All patients received primary radiotherapy or chemoradiation. The difference in received treatment regimens of these patients was predominantly caused by a change in treatment guidelines from standard radiotherapy to cisplatin-based chemoradiation in 1999 [1]. Clinicopathologic data of this historical cohort of patients, used in this study are summarized in table 1 [31,32].

Immunohistochemistry was performed to analyze expression levels of phospho-Ser139-H2AX (γ-H2AX), ATR, phospho-Ser33-RPA32 (pRPA32), DNA-PK catalytic subunit (DNA-PKcs), phospho-Ser2056-DNA-PKcs (pDNA-PKcs), Chk2, phospho-Thr68-Chk2 (pChk2), Chk1, phospho-Ser345-Chk1 (pChk1), MK2, phospho-Thr334-MK2 (pMK2). Detailed information on antibodies and immunohistochemical (IHC) staining protocols are provided in Supplemental Table 1. To validate IHC stainings, we used paraffin-embedded HeLa or CaSki cervical cancer cell lines treated with or without DNA damaging agents (cisplatin, ionizing irradiation, ultra-violet radiation) (Supplemental Figure 2). In order to validate antibodies for ATR, Chk1, Chk2, DNA-PKcs and MK2, we engineered HeLa cells stably expressing short-hairpin RNAs (shRNAs) targeted indicated proteins (Supplemental Figure 2 and Supplemental Table 2).

Each staining was semi-quantitatively scored, as previously described, by two independent observers (H.W.W. and either M.E./K.K.K./M.A.J.B) who were blinded for clinical data [31]. An immune reactivity score (IRS; 0-15) per sample was obtained by multiplying the score for the percentage of positively stained tumor cells (0 = 0%; 1 = 0-5%; 2 = 5-25%; 3= 25-50%; 4 = 50-75%; 5 = >75%) with the score for the staining intensity (0 = negative; 1 = weak; 2 = moderate; 3 = strong) (see Figure 1A). Cut-offs for γ-H2AX, Chk2 and pChk2 were based on literature, while other stainings were dichotomized (low *versus* high) by arbitrary cut-offs (see Supplemental Table 1) [50]. Cases with discordancy in IRS were re-evaluated to reach consensus. Patients were included for statistical analysis when ≥ 2 cores were evaluable. In 18.1-27.0% of the cases, less than 2 representative cores were available to determine an IRS.

Statistical analysis was performed with SPSS 22.0 for Windows. The use of specific statistical tests is explained in Supplemental Materials and Methods. DSS was defined as the time between diagnosis and death caused by cervical cancer or censored at last follow-up visit alive [31,32].

Cell lines and chemicals

The HPV-positive and p53 wild-type (wt) cervical cancer cell lines HeLa (HPV18), SiHa (HPV16) and CaSki (HPV16) were cultured in DMEM:Ham's F12 (1:1), supplemented with 10% of fetal calf serum (FCS), 100 U/mL of penicillin and 100 μg/mL of streptomycin. The primarily cervical squamous cell carcinoma cell line CSCC-7 and the cervical carcinoma cell lines CC-8, CC-11+ and CC10B were kindly provided by Dr. G.J. Fleuren (Leiden University Medical Center, The Netherlands) [51]. CC-8 and CC-10B cells were cultured in DMEM supplemented with 10% FCS and 100 U/mL of penicillin and 100 μg/mL of streptomycin. CSCC-7 and CC-11+ were cultured in DMEM supplemented with 20% FCS and 100 U/mL of penicillin and 100 μg/mL of streptomycin. Upon infection with shRNA virus, cells were continuously cultured in the presence of puromycin (1 μg/mL). Human embryonic 293T kidney cells (HEK293T) were cultured in DMEM supplemented with 10% FCS and 100 U/mL of penicillin and 100 μg/mL of streptomycin. Authenticity of cell lines was verified by DNA short-tandem repeat analysis (BaseClear, Leiden, The Netherlands).

If indicated, cells were irradiated using a CIS International/IBL 637 equipped with a $Cesium^{137}$ source (0.010124 Gy/second), or treated with cisplatin (1 μM, Tocris Biosciences), ATM inhibitor KU55993 (10 μM, Axon Medchem), ATR inhibitor NU6027 (10 μM, Sigma-Aldrich), DNA-PK inhibitor KU0060648 (1 μM, Axon Medchem) or MK2 inhibitor III (10 μM, Merck), Chk1/2 inhibitor AZD7762 (0.1 μM, Axon Medchem).

RNA interference

ShRNA sequences against human *CHEK1* (5'-CAACTTGCTGTGAATAGAG-3'), *ATR* (5'-GACGGTGTGCTCATGCGGC-3'), *MAPKAPK2* (5'-CAAGAGGACCCAGGAGAAA-3'), and *scrambled* negative control (5'-TTCTCCGAACGGTGCACGT-3') were cloned into pRetrosuper (pRS) [52]. The pRS-Chk2 plasmid [50], and HeLa cells, stably depleted of ATM were previously described [31]. ATM-GFP and SCR-GFP were provided by Dr. E.H. Blackburn (University of California, San Francisco, CA) and pSM2c-DNA-PKcs and pSM2c-Scrambled plasmids were kindly provided by Dr. A.S. Calkins (Dana Farber Cancer Institute, Boston, MA) and were previously described [53-54]. Retroviral particles were produced as described previously [55].

Western Blotting

Cell were lysed in Mammalian Protein Extraction Reagent (Thermo Scientific), supplemented with protease inhibitor and phosphatases inhibitor cocktail (#78440, Thermo Scientific). Thirty microgram of protein was used for SDS-PAGE. Separated proteins were transferred to polyvinylidene fluoride (PVDF) membranes and blocked in either 5% milk in Tris-buffered saline-0.01% Tween20 (TBS-T) or 3% bovine serum albumin (BSA) in TBS-T. Immunodetection was done with antibodies directed against ATM (#1549-1, rabbit, Epitomics), ATR (#sc-1887, goat, Santa Cruz Biotechnology), DNA-PKcs (#sc-9051, rabbit, Santa Cruz Biotechnology), MK2 (#3042, rabbit, Cell Signaling), Chk1 (#sc-56291, mouse, Santa Cruz Biotechnology), Chk2 (#sc-56297, mouse, Santa Cruz Biotechnology), β-actin (#A5441, mouse, Sigma-Aldrich). Horseradish peroxidase-conjugated antibodies (#P0448, #P0260, #P0449, DAKO) were used as secondary antibodies. Visualization was performed using Enhanced Chemiluminescence (Lumilight, Roche Diagnostics) and a Biorad Bioluminescence device, equipped with Quantity One/Chemidoc XRS software (Bio-rad Laboratories).

DSB repair assays

HeLa cells were stable transfected with the EJ5-GFP reporter as described previously [34]. The EJ5-GFP plasmid was a gift from Jeremy Stark (City of Hope, Duarte, CA, Addgene plasmid #44026) [34]. Monoclonal HeLa cells harboring the DR-GFP reporter were a gift from dr. J. Parvin (Ohio State University, Columbus, OH) and used as previously described [56]. Monoclonal HeLa-EJ5-GFP or HeLa-DR-GFP were transiently transfecting with I-SceI endonuclease using Lipofectamine 2000 (Invitrogen, Life Technologies). If indicated, 1 hour before transfection, cells were incubated with indicated concentrations of inhibitors. Forty-eight hours after transfection, GFP-positivity was quantified using flow cytometry on a FACS-Calibur (Becton Dickinson). A minimum of 10,000 events was analyzed per sample, and data was analyzed using CellQuest (Becton Dickinson) and Flowjo software.

MTT cytotoxicity assays

To measure short-term cytotoxicity 2,000 cells were plated in 96-well plates in the presence of indicated concentrations of cisplatin or inhibitors. After 3 days of treatment, 20 µL of 5 mg/mL 3-(4,5-dimethylthiazol-2-yl)-2,5-diphenyltetrazolium bromide (MTT) was added for 3 hours. Subsequently, culture medium was removed, and cells were incubated in 100 µL dimethyl

sulphoxide (DMSO) for 60 minutes. Absorbance was measured at 520 nm using an iMARK micoplate reader (Biorad Laboratories). Cytotoxicity was measured by calculating relative decreases in MTT conversion of treated versus untreated control cultures after subtraction of background absorbance.

Clonogenic survival assay

Depending on the amount of irradiation and/or cisplatin, different amounts of HeLa cells were plated in 6-well plates (Supplemental Table 3) and allowed to adhere for 24 hours. Subsequently, cells were left untreated or irradiated with 1, 2 or 4 Gy. If indicated, cells were treated for 4 hours with cisplatin prior to irradiation. DDR inhibitors were added 1 hour before radio- or chemotherapy. After 10-12 days, when colonies reached an approximate minimum size of 50 cells, colonies were fixed and stained as previously described [31].

Acknowledgments

We thank Drs Christian Reinhardt, Elizabeth Blackburn and Anne Calkins for contributing reagents. We are grateful to Dr. Henk Groen for help with statistical analysis. We thank colleagues of the Medical Oncology and Gynecological Oncology Departments for the helpful discussions. This work was supported by grants from the Dutch Cancer Society (RUG/NKB 2010-4833) and from the Netherlands Organization for Scientific Research (NWO-VIDI 016.136.334) to M.A.T.M.v.V. H.W.W. is supported by a fellowship of the Junior Scientific Masterclass from the University of Groningen. We thank the Van der Meer-Boerema Foundation for their support to H.W.W. and M.K.

References

1 Rose PG, Bundy BN, Watkins EB, Thigpen JT, Deppe G, Maiman MA, et al. Concurrent cisplatin-based radiotherapy and chemotherapy for locally advanced cervical cancer. N Engl J Med. 1999;340:1144–53.

2 Monk BJ, Tewari KS, Koh WJ. Multimodality therapy for locally advanced cervical carcinoma: state of the art and future directions. J Clin Oncol. 2007;25:2952–65.

3 Quinn MA, Benedet JL, Odicino F, Maisonneuve P, Beller U, Creasman WT, et al. Carcinoma of the cervix uteri. FIGO 26th annual report on the results of treatment in gynecological cancer. Int J Gynecol Obstet. 2006;95 Suppl 1:S43–103.

4 Bryant PE. Enzymatic restriction of mammalian cell DNA: evidence for double-strand breaks as potentially lethal lesions. Int J Radiat Biol Relat Stud Phys Chem Med. 1985;48:55–60.

5 Khanna KK, Jackson SP. DNA double-strand breaks: signaling, repair and the cancer connection. Nat Genet. 2001;27:247–54.

6 Roberts JJ, Thomson AJ. The mechanism of action of antitumor platinum compounds. Prog Nucleic Acid Res Mol Biol. 1979;22:71–133.

7 Pinto AL, Lippard SJ. Binding of the antitumor drug cis-diamminedichloroplatinum(II) (cisplatin) to DNA. Biochim Biophys Acta. 1985;780:167–80.

8 Eastman A. Activation of programmed cell death by anticancer agents: cisplatin as a model system. Cancer Cells. 1990;2:275–80.

9 Kelland L. The resurgence of platinum-based cancer chemotherapy. Nat Rev Cancer. 2007;7:573–84.

10 Kouass Sahbani K, Rezaee M, Cloutier P, Sanche L, Hunting DJ. Non-DSB clustered DNA lesions induced by ionizing radiation are largely responsible for the loss of plasmid DNA functionality in the presence of cisplatin. Chem Biol Interact. 2014;217:9–18.

11 Halazonetis TD, Gorgoulis VG, Bartek J. An oncogene-induced DNA damage model for cancer development. Science. 2008;319:1352–5.

12 Jackson SP, Bartek J. The DNA-damage response in human biology and disease. Nature. 2009;461:1071–8.

13 Kastan MB, Bartek J. Cell-cycle checkpoints and cancer. Nature. 2004;432:316–23.

14 Shiloh Y. ATM and related protein kinases: safeguarding genome integrity. Nat Rev Cancer. 2003;3:155–68.

15 Falck J, Coates J, Jackson SP. Conserved modes of recruitment of ATM, ATR and DNA-PKcs to sites of DNA damage. Nature. 2005;434:605–11.

16 Durocher D, Jackson SP. DNA-PK, ATM and ATR as sensors of DNA damage: variations on a theme? Curr Opin Cell Biol. 2001;13:225–31.

17 Abraham RT. Cell cycle checkpoint signaling through the ATM and ATR kinases. Genes Dev. 2001;15:2177–96.

18 Matsuoka S, Ballif BA, Smogorzewska A, McDonald ER 3rd, Hurov KE, Luo J, et al. ATM and ATR substrate analysis reveals extensive protein networks responsive to DNA damage. Science. 2007;316:1160–6.

19 Reinhardt HC, Aslanian AS, Lees JA, Yaffe MB. p53-deficient cells rely on ATM- and ATR-mediated checkpoint signaling through the p38MAPK/MK2 pathway for survival after DNA damage. Cancer Cell. 2007;11:175–89.

20 Reinhardt HC, Yaffe MB. Kinases that control the cell cycle in response to DNA damage: Chk1, Chk2, and MK2. Curr Opin Cell Biol. 2009;21:245–55.

21 Dyson N, Howley PM, Münger K, Harlow E. The human papilloma virus-16 E7 oncoprotein is able to bind to the retinoblastoma gene product. Science. 1989;243:934–7.

22 Werness BA, Levine AJ, Howley PM. Association of human papillomavirus types 16 and 18 E6 proteins with p53. Science. 1990;248:76–9.

23 Levine AJ. p53, the cellular gatekeeper for growth and division. Cell. 1997;88:323–31.

24 Suganuma M, Kawabe T, Hori H, Funabiki T, Okamoto T. Sensitization of cancer cells to DNA damage-induced cell death by specific cell cycle G_2 checkpoint abrogation. Cancer Res. 1999;59:5887–91.
25 Furgason JM, Bahassi el M. Targeting DNA repair mechanisms in cancer. Pharmacol Ther. 2013;137:298–308.
26 Chen BPC, Chan DW, Kobayashi J, Burma S, Asaithamby A, Morotomi-Yano K, et al. Cell cycle dependence of DNA-dependent protein kinase phosphorylation in response to DNA double strand breaks. J Biol Chem. 2005;280:14709–15.
27 Ben-Levy R, Leighton IA, Doza YN, Attwood P, Morrice N, Marshall CJ, et al. Identification of novel phosphorylation sites required for activation of MAPKAP kinase-2. EMBO J. 1995;14:5920–30.
28 Zhao H, Piwnica-Worms H. ATR-mediated checkpoint pathways regulate phosphorylation and activation of human Chk1. Mol Cell Biol. 2001;21:4129–39.
29 Matsuoka S, Rotman G, Ogawa A, Shiloh Y, Tamai K, Elledge SJ. Ataxia telangiectasia-mutated phosphorylates Chk2 *in vivo* and *in vitro*. Proc Natl Acad Sci U S A. 2000;97:10389–94.
30 Olson E, Nievera CJ, Klimovich V, Fanning E, Wu X. RPA2 is a direct downstream target for ATR to regulate the S-phase checkpoint. J Biol Chem. 2006;281:39517–33.
31 Roossink F, Wieringa HW, Noordhuis MG, Hoor ten KA, Kok M, Slagter-Menkema L, et al. The role of ATM and 53BP1 as predictive markers in cervical cancer. Int J Cancer. 2012;131:2056–66.
32 Noordhuis MG, Eijsink JJH, Hoor ten KA, Roossink F, Hollema H, Arts HJG, et al. Expression of epidermal growth factor receptor (EGFR) and activated EGFR predict poor response to (chemo)radiation and survival in cervical cancer. Clin Cancer Res. 2009;15:7389–97.
33 Darzynkiewicz Z, Bedner E, Traganos F. Difficulties and pitfalls in analysis of apoptosis. Methods Cell Biol. 2001;63:527–46.
34 Bennardo N, Cheng A, Huang N, Stark JM. Alternative-NHEJ is a mechanistically distinct pathway of mammalian chromosome break repair. PLoS Genet. 2008;4:e1000110.
35 Pierce AJ, Hu P, Han M, Ellis N, Jasin M. Ku DNA end-binding protein modulates homologous repair of double-strand breaks in mammalian cells. Genes Dev. 2001;15:3237–42.
36 Krajewska M, Fehrmann RSN, de Vries EGE, van Vugt MATM. Regulators of homologous recombination repair as novel targets for cancer treatment. Front Genet. 2015;6:96.
37 Beskow C, Kanter L, Holgersson A, Nilsson B, Frankendal B, Avall-Lundqvist E, et al. Expression of DNA damage response proteins and complete remission after radiotherapy of stage IB-IIA of cervical cancer. Br J Cancer. 2006;94:1683–9.
38 Xu J, Li Y, Wang F, Wang X, Cheng B, Ye F, et al. Suppressed miR-424 expression via upregulation of target gene Chk1 contributes to the progression of cervical cancer. Oncogene. 2013;32:976–87.
39 Cimprich KA, Cortez D. ATR: an essential regulator of genome integrity. Nat Rev Mol Cell Biol. 2008;9:616–27.
40 Manke IA, Nguyen A, Lim D, Stewart MQ, Elia AEH, Yaffe MB. MAPKAP kinase-2 is a cell cycle checkpoint kinase that regulates the G2/M transition and S phase progression in response to UV irradiation. Mol Cell. 2005;17:37–48.
41 Pomérance M, Quillard J, Chantoux F, Young J, Blondeau J-P. High-level expression, activation, and subcellular localization of p38-MAP kinase in thyroid neoplasms. J Pathol. 2006;209:298–306.
42 McShane LM, Altman DG, Sauerbrei W, Taube SE, Gion M, Clark GM. REporting recommendations for tumor MARKer prognostic studies (REMARK). Nat Clin Prac Oncol. 2005;2:416–22.
43 Bartkova J, Horejsí Z, Koed K, Krämer A, Tort F, Zieger K, et al. DNA damage response as a candidate anti-cancer barrier in early human tumorigenesis. Nature. 2005;434:864–70.

44 Gorgoulis VG, Vassiliou LV, Karakaidos P, Zacharatos P, Kotsinas A, Liloglou T, et al. Activation of the DNA damage checkpoint and genomic instability in human precancerous lesions. Nature. 2005;434:907–13.

45 Nuciforo PG, Luise C, Capra M, Pelosi G, d'Adda di Fagagna F. Complex engagement of DNA damage response pathways in human cancer and in lung tumor progression. Carcinogenesis 2007;28:2082–8.

46 Gamper AM, Rofougaran R, Watkins SC, Greenberger JS, Beumer JH, Bakkenist CJ. ATR kinase activation in G1 phase facilitates the repair of ionizing radiation-induced DNA damage. Nucleic Acids Res. 2013;41:10334–44.

47 Peasland A, Wang LZ, Rowling E, Kyle S, Chen T, Hopkins A, et al. Identification and evaluation of a potent novel ATR inhibitor, NU6027, in breast and ovarian cancer cell lines. Br J Cancer. 2011;105:372–81.

48 Foote KM, Blades K, Cronin A, Fillery S, Guichard SS, Hassall L, et al. Discovery of 4-{4-[(3R)-3-Methylmorpholin-4-yl]-6-[1-(methylsulfonyl)cyclopropyl]pyrimidin-2-yl}-1H-indole (AZ20): a potent and selective inhibitor of ATR protein kinase with monotherapy *in vivo* antitumor activity. J Med Chem. 2013;56:2125–38.

49 Fokas E, Prevo R, Pollard JR, Reaper PM, Charlton PA, Cornelissen B, et al. Targeting ATR *in vivo* using the novel inhibitor VE-822 results in selective sensitization of pancreatic tumors to radiation. Cell Death Dis. 2012;3:e441.

50 Alkema NG, Tomar T, van der Zee AGJ, Everts M, Meersma GJ, Hollema H, et al. Checkpoint kinase 2 (Chk2) supports sensitivity to platinum-based treatment in high grade serous ovarian cancer. Gynecol Oncol. 2014;133:591–8.

51 Koopman LA, Szuhai K, van Eendenburg JD, Bezrookove V, Kenter GG, Schuuring E, et al. Recurrent integration of human papillomaviruses 16, 45, and 67 near translocation breakpoints in new cervical cancer cell lines. Cancer Res. 1999;59:5615–24.

52 Brummelkamp TR, Bernards R, Agami R. Stable suppression of tumorigenicity by virus-mediated RNA interference. Cancer Cell. 2002;2:243–7.

53 Stohr BA, Blackburn EH. ATM mediates cytotoxicity of a mutant telomerase RNA in human cancer cells. Cancer Res. 2008;68:5309–17.

54 Sand-Dejmek J, Adelmant G, Sobhian B, Calkins AS, Marto J, Iglehart DJ, et al. Concordant and opposite roles of DNA-PK and the "facilitator of chromatin transcription" (FACT) in DNA repair, apoptosis and necrosis after cisplatin. Mol Cancer. 2011;10:74.

55 van Vugt MATM, Gardino AK, Linding R, Ostheimer GJ, Reinhardt HC, Ong SE, et al. A mitotic phosphorylation feedback network connects Cdk1, Plk1, 53BP1, and Chk2 to inactivate the G(2)/M DNA damage checkpoint. PLoS Biol. 2010;8:e1000287.

56 Krajewska M, Fehrmann RSN, Schoonen PM, Labib S, de Vries EGE, Franke L, et al. ATR inhibition preferentially targets homologous recombination-deficient tumor cells. Oncogene. 2014;34:3474-81.

Supplementals

Supplemental materials and Methods

Patient group and immunohistochemistry

Between January 1980 and December 2006, 489 patients were diagnosed with cervical cancer (International Federation of Gynecology and Obstetrics (FIGO) stage IB1 to IVA) and primarily treated with radiotherapy or chemoradiation in the University Medical Center Groningen (UMCG) and affiliated hospitals. Patients with stage IVB were excluded, as their management plan was individualized (for patient flow chart see Supplemental Figure 1). In 375 cases, sufficient tumor tissue was available to retrospectively construct a tissue microarray (TMA) construction, as previously described [31,51]. Patient tissues were divided over 7 TMAs. One TMA (n = 49) was excluded due to extensive core loss. Compared to this latter TMA, the remaining evaluable patients (n = 326) were more recently diagnosed with cervical cancer (P <0.001, Spearman's rho; median: 1991 *vs* 1998) and were less frequently treated with primarily radiotherapy (P <0.001).

Treatment details were previously reported [51]. In short, standard radiotherapy regime consisted of external beam radiotherapy (up to 45 Gy) combined with low-dose-rate brachytherapy (twice 17.5 Gy). Before 1999, chemotherapy consisted of three cycles of carboplatin and 5-fluorouacil, while after 1999 a weekly dose of 40mg/m2 cisplatin was intravenously administered for 6 consecutive weeks. Tumor tissues were part of staging biopsies prior to treatment. When acquired, tissue specimens were formalin-fixed, paraffin-embedded and stored at room temperature. FIGO guidelines were used for staging. A gynaecological pathologist determined tumor grade and classification. All patients provided informed consent for data collection and tumor tissue storage. Data of clinical parameters and follow-up were prospectively collected in a central database, which was solely accessible by two designated data managers. For this retrospective analysis an anonymized dataset was retrieved from the central database. Further institutional review board approval was not needed according to Dutch law.

When acquired, tissue specimens were formalin-fixed, paraffin-embedded and stored at room temperature. Staging was classified according the International Federation of Gynecologists and Obstetricians (FIGO) criteria. A gynaecological pathologist determined tumor grade and classification. All patients provided informed consent for data collection and tumor tissue storage. Data of clinical parameters and follow-up were prospectively collected in a central database, which was solely accessible by two designated data managers. For this retrospective study an anonymized dataset was retrieved from the central database. We could only include 326 patients (FIGO IB1-IVA), as one TMA (n = 49) suffered from core loss and insufficient remaining tumor tissues of these patients limited re-construction of the TMA. Treatment strategy was in 152 cases primarily radiotherapy (46.6%), whereas in 174 cases (53.4%) primarily chemoradiotherapy was given. Radiation regimes used were external beam radiotherapy (max. 45 Gy) and low-dose rate brachytherapy. Before 1999, chemotherapy consisted of three cycles of carboplatin and 5-fluorouacil. After 1999, the chemotherapeutic regime consisted of a weekly dose of 40 mg/m2 cisplatin intravenously for 6 consecutive weeks concurrent with external pelvic and intracavitary radiotherapy. Biopsy specimens taken 8 to 10 weeks after completion of radio-/chemotherapy or material from hysterectomy were available in 250 out of 326 cases (76.7%) to evaluate response to therapy.

In short, for immunohistochemistry 3 µm TMA sections were mounted on amino-propyl-ethoxy-silan-coated slides and deparaffinized using xylene. Slides were incubated for 30 minutes in 0.3% hydrogen peroxidase to block endogeneous peroxidase. Visualization of staining was done using 3,3-diaminobenzidine (DAB) and haematoxyline was used as counterstaining. More details are summarized in Supplemental Table 1. To validate stainings for phosphorylated proteins we used not only paraffin-embedded HeLa or CaSki cervical cancer cell lines, but also human tissue slides of ovarian cancer, colon cancer, breast cancer and normal testis as positive controls (Supplemental Figure 2). For validation of antibodies against ATR, Chk1, Chk2, DNA-PKcs and MK2, we used human tissue of ovarian, colon and breast cancers as positive controls (Supplemental Figure 2).

An overview of clinic-pathological data is summarized in Table 1. Median follow-up time was 4.0 (range: 0.1-18.4) years for all 326 LACC patients. For patients primarily treated with radiotherapy (n = 152) or chemoradiation (n = 174) follow-up was not significantly different (median 3.1 *vs.* 4.9; $P = 0.123$). Patients treated with primarily chemoradiation were younger compared to patients who received radiotherapy alone (median 47.4 *vs.* 65.6; $P < 0.001$). All other baseline characteristics were not significantly different between both groups (data not shown). The associations between treatment groups (radiotherapy and/or chemoradiation) with patient characteristics were tested with Pearson's chi-square test, Fisher's exact test or logistic regression when appropriate. Continuous variables (age and follow-up) were tested with a non-parametric test, Spearman's rho. Pearson's chi-square test or Fisher's exact test were used to test associations between stainings. Survival analysis was performed using the Cox proportional hazard regression model. For multivariate analyses, only variables with a *P*-value <0.10 were included. *P*-values of <0.05 were considered statistically significant.

RNA interference

Retroviral particles were produced by transfecting HEK293T with either pRS or pSM2c plasmids along with the packaging plasmids pMDG/P and pMDG in a 3:2:1 ratio using a calcium phosphate protocol. Virus-containing supernatant culture medium filtered (0.22 µM; Millipore), mixed with polybrene (4 µg/mL) and used for infection for single infection of the indicated target cells. Twenty-four hours after the third infection, puromycin was added (1 µg/mL) for selection. For production of lentiviral particles, a similar protocol was used except that the lentiviral packaging plasmids pCMV-R8.2 and pCMV-VSGV were used, followed by GFP-based sorting of infected cells.

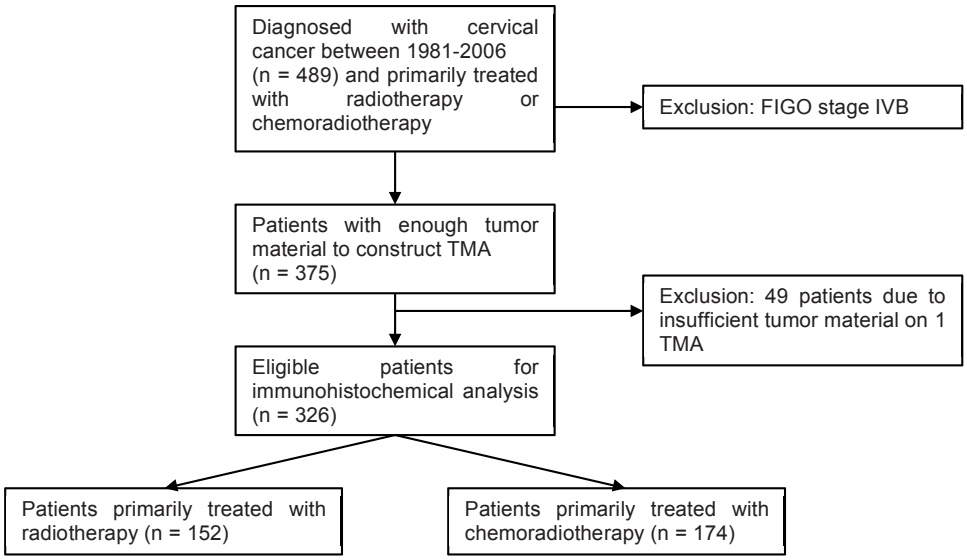

Supplemental Figure1: Patient selection for IHC analysis *Flow diagram indicating selection of patients included for retrospective analysis.*

Supplemental Figure 2: Overview of immunohistochemical control stainings on human tissue and paraffin-embedded cervical cancer cell lines. (A) *Positive controls for immunohistochemical stainings on normal and selected human cancer tissues.* ***(B)*** *Representative immunohistochemical stainings of paraffin-embedded cervical cancer cell lines (HeLa and CaSki) used as positive and negative controls. To validate stainings with indicated phospho-specific antibodies, cancer cell lines were treated with or without DNA damaging agents (10 μM cisplatin, 5 Gy ionizing radiation, 50 J/m^2 ultra-violet (UV) radiation). To validate immunohistochemical stainings for ATR, DNA-PKcs and Chk1, HeLa cells stably expressing indicated shRNAs were processed for immunoblotting. In parallel, cell lines were paraffin-embedded, and processed for immunohistochemical staining.*

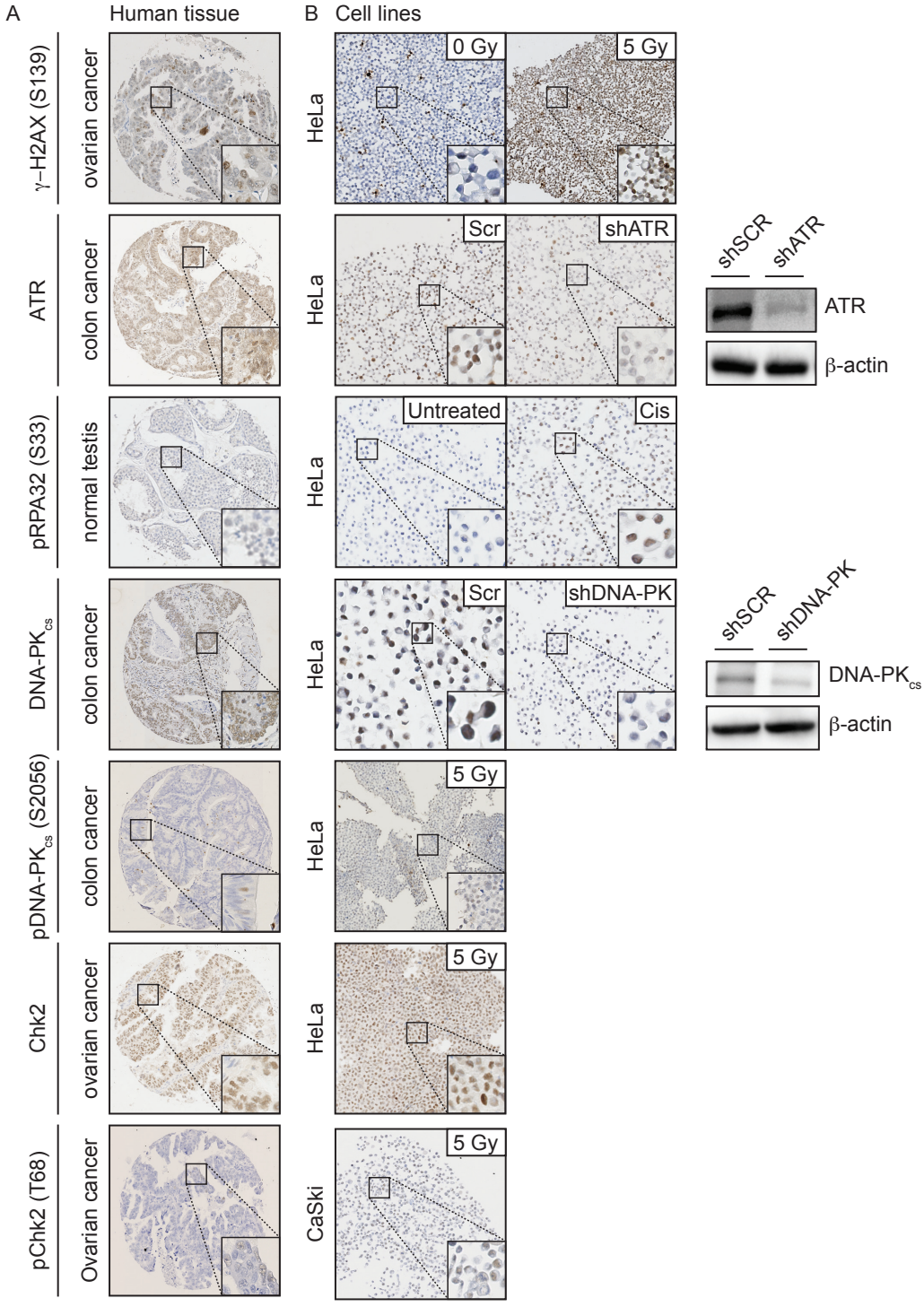
A
Human tissue
B
Cell lines
γ–H2AX (S139)
ovarian cancer
ATR
colon cancer
pRPA32 (S33)
normal testis
DNA-PKcs
colon cancer
pDNA-PKcs (S2056)
colon cancer
Chk2
ovarian cancer
pChk2 (T68)
Ovarian cancer
HeLa
0 Gy
5 Gy
HeLa
Scr
shATR
HeLa
Untreated
Cis
HeLa
Scr
shDNA-PK
HeLa
5 Gy
HeLa
5 Gy
CaSki
5 Gy
shSCR
shATR
ATR
β-actin
shSCR
shDNA-PK
DNA-PKcs
β-actin

Supplemental Table 1: Details of antibodies used for immunohistochemical analysis and arbitrary cut-offs used for statistical analysis.

Target	Brand	Catalogue No.	Antigen retrieval	Dilution	Incubation time	Detection method	IRS cut-off
γH2AX	Millipore	05-636	Citrate (pH 6.0)	1:300	60 minutes RT	RAMpo- GARpo	≥ 2
ATR	Abcam	ab110883	Citrate (pH 6.0)	1:50	60 minutes RT	GARpo- RAGpo	≥ 12
pRPA32	Bethyl	A300-246A	TRIS/HCL (pH 9.0)	1:1500	60 minutes RT	Avidin- biotin	≥ 4
DNA-PKcs	Santa Cruz	sc9051	Citrate (pH 6.0)	1:200	60 minutes RT	GARpo- RAGpo	≥ 9
pDNA-PKcs	Abcam	ab124918	TRIS/HCL (pH 9.0)	1:50	60 minutes RT	GARpo- RAGpo	≥ 1
Chk1	Epitomics	1740-1	EDTA (pH 8.0)	1:50	60 minutes RT	GARpo- RAGpo	≥ 6
pChk1	Cell signaling	2348	TRIS/HCL (pH 9.0)	1:50	o/n 4ºC	GARpo- RAGpo	≥ 1
Chk2	Santa Cruz	sc56297	TRIS/EDTA (pH 9.0)	1:100	60 minutes RT	RAMpo- GARpo	≥ 12
pChk2	Cell signaling	2197	Citrate (pH 6.0)	1:50	o/n 4ºC	Avidin- biotin	≥ 1
MK2	Abcam	ab63574	Citrate (pH 6.0)	1:200	60 minutes RT	GARpo- RAGpo	≥ 2
pMK2	Cell signaling	3041	TRIS/HCL (pH 9.0)	1:50	o/n 4ºC	GARpo- RAGpo	≥ 8

IRS = immunoreactive score; TRIS = tris(hydroxymethyl)aminomethane; HCL = hydrochloric acid; EDTA = ethylenediaminetetraacetic acid; No. = number; RT = room temperature; RAMpo = Rabbit Anti-Mouse horseradish peroxidase; GARpo = Goat Anti-Rabbit horseradish peroxidase; RAGpo = Rabbit Anti-Goat horseradish peroxidase; o/n = overnight.

Supplemental Table 2: shRNA sequences against human ATR, DNA-PKcs and CHEK1.

Target	shRNA sequence	Reference
ATR	5'-GACGGTGTGCTCATGCGGC-3'	-
DNA-PKcs	5'-GATCG CACCTTACTCT GTT-3'	-
CHEK1	5'-CAACTTGCTGTGAATAGAG-3'	Krause[1]
Scramble	5'-TTCTCCGAACGGTGCACGT-3'	Park[2]

[1] Krause DR, Jonnalagadda JC, Gatei MH, Sillje HH, Zhou BB, Nigg EA, Khanna K. Suppression of Tousled-like kinase activity after DNA damage or replication block requires ATM, NBS1 and Chk1. Oncogene 2003: 4;22:5927-37.
[2] Park SY, Yu X, Ip C, Mohler JL, Bogner PN, Park YM. Peroxiredoxin 1 interacts with androgen receptor and enhances its transactivation. Cancer Res: 67:9294-303.

Supplemental Table 3: Density of cells plated per well for clonogenic survival assay.

IR (Gy)	0	1	2	4	0	1	2	4
Compound	**No cisplatin**				**Cisplatin**			
Untreated	100	250	500	500	100	500	500	500
DMSO	100	250	500	500	100	500	500	500
KU55933	100-1,000	500-5,000	1,000-5,000	1,000-5,000	100-1,000	500-5,000	1,000-5,000	1,000-5,000
NU6027	100-1,000	500-5,000	1,000-5,000	1,000-5,000	100-1,000	500-5,000	1,000-5,000	1,000-5,000
AZD7762	100-1,000	500-5,000	1,000-5,000	1,000-5,000	100-1,000	500-5,000	1,000-5,000	1,000-5,000
KU0060648	100-1,000	500-5,000	1,000-5,000	1,000-5,000	100-1,000	500-5,000	1,000-5,000	1,000-5,000
MK2-inhibitor III	100-1,000	500-5,000	1,000-5,000	1,000-5,000	100-1,000	500-5,000	1,000-5,000	1,000-5,000

IR: ionizing radiation; cisplatin (1 μM); KU55993 (10 μM); NU6027 (10 μM); AZD7762 (0.1 μM); KU0060648 (0.1 μM); MK2 inhibitor III (10 μM)

Supplemental Table 4: Association between the expression pattern and activation status of γ-H2AX, ATR, pRPA32, DNA-PK$_{cs}$, pDNA-PK$_{cs}$, Chk1, pChk1, Chk2, pChk2, MK2, pMK2 in cervical cancer patients treated with primary radiotherapy (n=152) or primary chemoradiotherapy (n=174).

Primary radiotherapy

	ATR	pRPA2	DNA-PKcs	pDNA-PKcs	Chk1	pChk1	Chk2	pChk2	MK2	pMK2
γ-H2AX	0.558	0.022	0.458	0.003	0.004	0.043	0.100	<0.001	0.475	<0.001
ATR		0.115	0.200	0.293	<0.00	0.015	0.447	0.028	0.465	0.002
pRPA32			0.652	0.060	<0.00	<0.00	0.791	0.001	0.310	<0.001
DNA-PKcs				0.134	0.086	0.769	0.324	0.874	0.908	0.329
pDNA-PKcs					0.009	<0.00	0.031	0.002	0.123	0.002
Chk1						<0.00	0.118	<0.001	0.231	<0.001
pChk1							0.783	0.002	0.301	<0.001
Chk2								<0.001	0.657	0.200
pChk2									0.178	0.001
MK2										0.109

Primary chemoradiation

	ATR	pRPA2	DNA-PKcs	pDNA-PKcs	Chk1	pChk1	Chk2	pChk2	MK2	pMK2
γ-H2AX	0.627	0.126	0.418	0.045	0.024	0.002	0.576	0.064	0.861	0.033
ATR		0.597	0.359	0.896	0.325	0.287	0.290	0.485	0.975	0.326
pRPA32			<0.001	0.007	0.520	<0.00	0.726	0.180	0.054	0.052
DNA-PKcs				<0.001	0.143	0.001	0.949	0.134	0.516	0.055
pDNA-PKcs					0.171	0.005	0.035	0.041	0.204	0.111
Chk1						0.006	0.749	0.129	0.536	0.127
pChk1							0.553	0.130	0.096	0.001
Chk2								0.016	0.844	0.325
pChk2									0.396	0.006
MK2										0.001

Values summarized in tables indicate the P-values

Supplemental Table 5: Potentiation of cisplatin by specific DDR inhibitors in different cervical cancer cell lines.

Target			Primary cervical cancer cell lines			
	HeLa	SiHa	CSCC-7	CC-8	CC-10B	CC-11+
ATMi	0.0960	0.2624	<0.0001	0.8905	<0.0001	<0.0001
ATRi	<0.0001	<0.0001	0.0155	<0.0001	0.0002	0.3344
DNA-PKi	0.5522	0.3882	0.0001	0.5345	0.0014	0.0060
Chk1/2i	<0.0001	<0.0001	<0.0001	0.0202	<0.0001	<0.0001
MK2i	0.7822	n/a	0.6808	0.2502	<0.0001	0.0026
VE-821	n/a	n/a	<0.0001	<0.0001	<0.0001	0.0596
Chk2i	0.3019	0.1178	n/a	n/a	n/a	n/a

Values demonstrated in the table are the P-values from the extra sum-of-square F-test in which the difference of the curves between control and DDR inhibitor are tested. CSCC-7: cervical squamous cell carcinoma 7: CC-8: cervical carcinoma 8; CC-10B: cervical carcinoma 10B; CC-11+: cervical carcinoma 11+; ATMi: KU-55933; ATRi: NU6027; DNA-PKi: KU0060648; Chk1/2i: AZD7762; MK2I: MK2 inhibitor III; Chk2i: Chk2-inhibitor; n/a: not available.